ISET Journal of Earthquake Technology, Paper No. 514, Vol. 48, No. 1, March 2011, pp. 11–27

HEALTH ASSESSMENT OF STRUCTURES EXPOSED TO SEISMIC EXCITATIONS

Ajoy Kumar Das and Achintya Haldar
Department of Civil Engineering & Engineering Mechanics
University of Arizona
Tucson, AZ 85721, U.S.A.

ABSTRACT

The health assessment of existing infrastructure just after an earthquake is a very important but challenging task. Even engineered structures can suffer significant damage(s) due to seismic excitations. To ensure public safety and to maintain the economic activities of the surrounding communities, structural health needs to be assessed promptly following an earthquake. Two novel structural health assessment procedures are under development at the University of Arizona. They are known as the modified iterative least-squares with unknown input (MILS-UI) and generalized iterative least-squares extended Kalman filter with unknown input (GILS-EKF-UI) techniques. These procedures are finite-element based time domain system identification (SI) techniques, which are capable of identifying structures at the element level by using only the dynamic response information. These procedures have been extensively verified by using the numerically simulated and laboratory measured response information, as obtained for the defect-free and defective frames under sinusoidal and impulsive excitations. The health assessment of the same defect-free and defective frames by using the numerically simulated response information under seismic excitations is presented here.

KEYWORDS: Earthquake Ground Motion, Finite Element, System Identification, Structural Health Assessment

INTRODUCTION

The health assessment of an engineered civil infrastructure just after strong earthquakes is very important for quickly developing post-disaster mitigation plans in the most economical way, without exposing the public to excessive risk. The mitigation plans may include opening them to public with or without some restrictions of their uses, inspecting them more frequently, repairing the identified defective members, or of replacing the whole structure. As recommended in many standards and practiced widely, visual inspections are primarily used to assess structural health and to develop the remedial actions as necessary. However, a visual inspection does not consider structural performance at the current deteriorated state. Thus, it cannot provide a quantitative assessment of the structural health. This deficiency reduces its effectiveness to assess structural health in many different ways, including the importance of a member in the overall structural integrity, redundancy in the load transfer path, load carrying capacity of the member during the ground excitations, lack of accessibility to inspect the member or the defects that may be hidden behind the obstructions, and the prior history of damage that might have been caused during the installation and/or due to the accidental loads. Also, visual inspections may require an excessive amount of resources in some cases, for example, in inspecting a bridge over a river.

Damages that change structural behaviour may not always be visible with the naked eye. During the 1994 Northridge earthquake, welds got fractured in the moment-resisting steel frames. Similarly, welds got fractured during the 1989 Loma Prieta earthquake, but those remained undetected for a long period, thus exposing the users of these buildings to an additional risk. If the locations of defective spots are known, we have technological sophistication to inspect them, when we use localized experimental techniques, such as acoustic, ultrasonic, magnetic-field, radio-graphs, eddy-current, thermal-field methods. These techniques can also be used to inspect different types of structures, including the marine offshore structures, aerospace structures, etc. However, they may not be appropriate to inspect a complex civil infrastructure consisting of high-rise buildings, long-span bridges with complex arrangements, industrial structures, etc., since the locations of defects are unknown in such cases. An objective nondestructive procedure is therefore urgently needed for the rapid assessment of structural health.

Numerous damage detection philosophies have been developed during the last three decades. They are effectively summarized in several state-of-the-art papers (Lew et al., 1991; Ghanem and Shinozuka, 1995; Shinozuka and Ghanem, 1995; Doebling et al., 1996; Housner et al., 1997; Humar et al., 2006; Kerschen et al., 2006; Worden et al., 2007; Worden et al., 2008; Ahmed, 2009). Due to its many advantages, structural health assessment (SHA) using dynamic response information has recently become very popular in the research community. Its basic philosophy is based on the concept that the damage(s) that cause changes in the structural dynamical behaviour or responses can be characterized by using an inverse identification procedure, known as the system identification (SI) technique. There are three basic components in a vibration-based SI technique, namely, (i) input time-varying loading or excitation, (ii) the system that needs to be identified, assuming that it can be represented by a series of equations in terms of its parameters, such as mass, stiffness and damping properties, and (iii) the output structural dynamic responses measured by the sensors. The main objective here is to obtain information on the system parameters by using only the output dynamic responses. The information on the input excitation may or may not be necessary. Many vibration-based SI procedures have already been developed; their relative merits and demerits are available in the literature (Wang and Haldar, 1994).

When the dynamic responses of a system are employed for parameter identification, the response information can be processed either in the frequency domain or in the time domain. In general, the frequency-domain procedures are relatively simpler and have, therefore, been widely used in the past. They can assess structural health in the global sense, i.e., they can answer whether the structure is defective or not, but they cannot identify the location or the severity of defects. This prompted the researchers, including the authors and their research team, to detect defects at the local element level by using different time-domain numerical procedures, including the recursive techniques, maximum likelihood techniques, etc. In any case, SHA can be broadly conducted at four different Levls (Rytter, 1993), namely, Level 1 consisting of the determination of the presence of damage in a structure, Level 2 consisting of the determination of geometric location of the damage, Level 3 consisting of the quantification of the severity of the damage, and Level 4 consisting of the prediction of the remaining service life of the structure. Levels 1, 2 and 3 are specifically addressed in this paper. In general, the procedure used should be simple, inexpensive, and easy-to-implement for a quick SHA.

Two novel structural health assessment procedures are under active development by a research team at the University of Arizona, which will satisfy the first three levels of SHA. They are finite-element based time-domain SI techniques, which can assess the health of structures at the element level by using only the noise-contaminated dynamic response information and without using any information on the input excitation, thus increasing the implementation potential of these techniques. These procedures are conceptually based on the minimization of errors in the identified parameters. A least-squares based procedure, called as the iterative least-squares with unknown input (ILS-UI) method, was initially developed by Wang and Haldar (1994) for the situation when dynamic response information is available at all the dynamic degrees of freedom (DDOFs). They considered viscous damping in the governing equations of motion and identified damping for all the members in a structure. Since the changes in damping caused by different levels of defects are not known clearly at present, and to improve the efficiency of the algorithm, a Rayleigh-type (i.e., mass- as well as stiffness-proportional) damping instead of viscous damping can be used without compromising the damage detection capability. This is called as the modified iterative least-squares (MILS-UI) method (Ling and Haldar, 2004; Katkhuda et al., 2005). For a structure consisting of m structural elements, the ILS-UI procedure will identify m damping parameters, but these parameters will be only two if the MILS-UI method is used. The MILS-UI method significantly improves the efficiency of the algorithm, particularly for the large structural systems. Since the response information may not be available at all the DDOFs, particularly for the large real structures, later Wang and Haldar (1997) successfully exploited the ability of the extended Kalman filter (EKF) technique to identify a structure by using the minimum response information, developed a new technique by combining EKF with the ILS-UI method, and called it as the ILS-EKF-UI method. Several improvements were incorporated later into this method to increase its computational efficiency and to make it applicable for the health assessment of real structures. This is now known as the generalized iterative least-squares extended Kalman filter with unknown input (GILS-EKF-UI) method (Katkhuda and Haldar, 2008; Haldar, 2009). It is necessary to emphasize that the EKF-based procedures have been used over the years for structural identification by using their standard form (Hoshiya and Saito, 1984; Koh et al., 1991; Hoshiya and Sutoh, 1993; Oreta and Tanabe, 1993, 1994; Maruyama and Hoshiya, 2001; Corigliano and Mariani, 2004; Ghanem and Ferro, 2006; Wu and Smyth, 2007). Recently, a few

slightly varied forms of the EKF method (Yang et al., 2006, 2007; Ghosh et al., 2007; Zhou et al., 2008; Saha and Roy, 2009) have also been used for SHA. The proposed GILS-EKF-UI procedure uses the standard EKF form for SHA by using the minimum response information.

The ILS-UI and MILS-UI procedures were extensively verified by using the numerically simulated response information for the fixed-ended and simply-supported one-dimensional beams (Vo and Haldar, 2004). In this approach, the computer-generated response information was used to identify the defect-free and defective beams excited by the sinusoidal loading. After the completion of this phase, the health of the beams was successfully assessed by using the experimental responses obtained in a laboratory (Vo and Haldar, 2008a, 2008b). After the verification of the ILS-UI and MILS-UI methods for one-dimensional beams, this study was extended to identify the health of a two-dimensional frame. As will be discussed in more detail later, the responses of steel frame to sinusoidal and impulsive loadings were numerically simulated by using a commercially available computer program. Defects of several types were then introduced in the frame. The MILS-UI and GILS-EKF-UI methods were verified by using the analytical response information (Katkhuda, 2004; Katkhuda et al., 2005; Katkhuda and Haldar, 2006; Haldar and Das, 2010), as obtained for the health assessment of the undamaged and damaged configurations. A one-third scale model of the frame was then built and the health assessment capabilities of the two methods were studied by conducting extensive laboratory investigations for the sinusoidal and impulsive loadings applied at the super-structure. By using the so-obtained experimental response information, the health of the frame was assessed for its undamaged and damaged configurations (Martinez-Flores, 2005; Martinez-Flores and Haldar, 2007; Martinez-Flores et al., 2008; Haldar et al., 2008). Since it was not possible in our laboratory to excite the frame by a seismic loading applied at its base, this paper mainly focuses on the theoretical verification of both methods by using the numerically simulated responses of the frame under a seismic excitation and on the confirmation of the observations already made during the laboratory investigations with other types of loadings. The responses are numerically simulated by using the commercially available ANSYS software. For the ease of presentation, the theoretical concepts behind the MILS-UI and GILS-EKF-UI methods are briefly discussed below.

MATHEMATICAL CONCEPT OF MILS-UI PROCEDURE

The governing differential equations of motion of a linear multi-degree-of-freedom system under an earthquake excitation can be written in matrix notation as

$$[M]\{\ddot{x}(t)\}+[C]\{\dot{x}(t)\}+[K]\{x(t)\}=-[M]\{I\}\{\ddot{u}_g(t)\} \tag{1}$$

where $[M]$ is the global mass matrix, $[C]$ is the viscous damping matrix, $[K]$ is the global stiffness matrix, $\{I\}$ is the unit vector, and $\{\ddot{u}_g(t)\}$ is the ground-acceleration time-history vector. As discussed earlier, in the MILS-UI method, the damping is considered to be (mass- and stiffness-proportional) Rayleigh damping and therefore it can be represented as $(\alpha[M]+\beta[K])$, where α and β are the Rayleigh damping coefficients, and $\{\ddot{x}(t)\}$, $\{\dot{x}(t)\}$ and $\{x(t)\}$ are the vectors containing the dynamic responses in terms of acceleration, velocity and displacement, respectively, relative to the base at the time *t*. The global mass and stiffness matrices can be formed by using the standard finite element procedure. As in the other SI methods, the mass matrix $[M]$ is assumed to be known. Since it is impractical to know the exact time history of the earthquake ground acceleration soon after the excitation, it is considered to be unknown. The parameters to be identified are the stiffness parameters in $[K]$ and the damping coefficients, α and β. To this end, Equation (1) can be reorganized as

$$[A(t)]_{nm\times h}\{D\}_{h\times 1}=\{F(t)\}_{nm\times 1} \tag{2}$$

For the over-determined system represented by Equation (2), $[A(t)]$ is a rectangular matrix with the number of rows, *nm*, greater than the number of columns, *h*, and is populated with the responses at all the DDOFs in terms of displacement vector $\{x(t)\}$ and velocity vector $\{\dot{x}(t)\}$ at the time *t*; $\{D\}$ is a

vector composed of the unknown system parameters (i.e., the stiffness and damping coefficients) to be identified; $\{F(t)\}$ is a vector composed of the unknown input ground excitation and the inertia forces at the time *t*; h is the total number of unknown parameters to be identified; nm is equal to $n \times m$; n is the total number of DDOFs; and m is the total number of the time points of the response measurements.

The system parameter vector $\{D\}$ in Equation (2) can be defined as

$$\{D\}_{h\times 1} = [k_1, k_2, ..., k_{ne}, \beta k_1, \beta k_2, ..., \beta k_{ne}, \alpha]^{\mathrm{T}} \tag{3}$$

where h is equal to $2ne+1$; ne is the total number of finite elements; k_i is the stiffness parameter of the ith element and is defined as $E_i I_i / L_i$, where L_i and I_i are respectively the length and the second moment of inertia of the cross-section of the member, and E_i is the Young's modulus of elasticity of the material. To solve for $\{D\}$, the least-square technique is used to minimize the total error Er in the identification of the structure, i.e.,

$$Er = \sum_{r=1}^{n\times m}\left(F_r - \sum_{s=1}^{h} A_{rs}(t) D_s\right)^2; \quad r = 1, 2, \ldots, n\times m \tag{4}$$

To minimize the total error, Equation (4) is differentiated with respect to each one of the D_i parameters as

$$\frac{\partial Er}{\partial D_i} = \sum_{r=1}^{n\times m}\left(F_r - \sum_{s=1}^{h} A_{rs} D_s\right) A_{ri} = 0; \; i = 1, 2, \ldots, h \tag{5}$$

Equation (5) gives h simultaneous equations, the solution of which will give the estimation of all the h unknown parameters. The unknown parameters can be evaluated as

$$\{D\}_{h\times 1} = \left([A]^{\mathrm{T}}_{h\times nm}[A]_{nm\times h}\right)^{-1}[A]^{\mathrm{T}}_{h\times nm}\{F\}_{nm\times 1} \tag{6}$$

The system parameter vector $\{D\}$ can be solved, provided the force vector $\{F(t)\}$ and matrix $[A(t)]$ are known. However, since the input ground excitation is not known, the force vector $\{F(t)\}$ in Equation (2) becomes an unknown. The MILS-UI method solves for the vector $\{D\}$ by starting an iterative process, where the unknown input seismic excitation is assumed to be zero at all time points (Katkhuda et al., 2005). This assumption guarantees a non-singular solution of Equation (2), without compromising the convergence or the accuracy of the method. It is observed that the method is not sensitive to this initial assumption. It may be emphasized that the fully populated square matrix $[A]^{\mathrm{T}}[A]$ has full rank and does have an inverse. In Equation (6), $\left([A]^{\mathrm{T}}[A]\right)^{-1}[A]^{\mathrm{T}}$ is called as the pseudo inverse of matrix $[A]$.

The major drawback of the MILS-UI procedure is that it requires responses to be observed at all DDOFs. This may not be possible for large structures with numerous DDOFs. Also, the presence of noise in the measured responses is not explicitly addressed by the MILS-UI method. To increase the implementation potential of this method, so that it is able to identify large complicated structural systems, the GILS-EKF-UI method is proposed below.

MATHEMATICAL CONCEPT OF GILS-EKF-UI PROCEDURE

The basic objective of the GILS-EKF-UI method is to identify large structural systems by using only the noise-contaminated response measured at a small part of the structure. This will be discussed in more detail in the section on verification, for the situation when the health of a two-dimensional frame shown in Figure 1 needs to be assessed. The finite-element representation of the frame is shown in Figure 2(a). Responses are measured only at a small part of the frame, denoted hereafter as the substructure and shown

in Figure 2(b). The substructure consists of three nodes, i.e., Nodes 1, 2, and 3, and two elements, i.e., Beam 1 and Column 4. Our task is to identify the whole frame by using the responses measured at the three nodes. It will be shown that the GILS-EKF-UI method can be used for this purpose. It may be pointed out that in a real inspection accelerometers are used to measure the responses. The required information on velocity and displacement time histories is then obtained by successively integrating the measured acceleration time histories (Vo and Haldar, 2003). The issues related to noise-contaminated acceleration time histories have been discussed by Vo and Haldar (2003).

Fig. 1 Three-story experimental frame

The Kalman filter (KF)-based methodologies (Jazwinski, 1970; Maybeck, 1979; Welch and Bishop, 1995) can be used if response information is not available at all the DDOFs; however, in order to implement these methodologies, the information on input excitation and the initial state vector must be available. The extended Kalman filter method with weighted global iteration (EKF-WGI) proposed by Hoshiya and Saito (1984) also requires similar information; however, it can only identify mildly nonlinear systems. In any case, with the requirements of additional information, the basic KF-based formulation will not satisfy the main objective of this study. To circumvent this situation, the desirable features of the MILS-UI and EKF metods are integrated and a two-stage approach is proposed, leading to the development of the GILS-EKF-UI method. In Stage 1, based on the available response information, a substructure is considered that will satisfy all the requirements of the MILS-UI method. At the completion of Stage 1, the time history of the unknown excitation force, the Rayleigh-damping coefficients, and the stiffness parameters of all the elements in the substructure will be available. The information obtained on damping will be applicable to the whole structure. Further, the stiffness parameters identified for the substructure can be judiciously used to develop the initial state vector of the stiffness parameters for the whole structure. The generated information will thus satisfy all the requirements to implement the EKF-based concept, and therefore in Stage 2, the whole structure can be identified by using only a limited noise-contaminated response information.

The location and size of substructure are to be selected based on the available measured responses. For economic reasons, the size of substructure should be kept to a minimum. The past maintenance history of the structure being inspected or the experience of inspectors in dealing with a particular type of structure may also help in selecting the location of the substructure appropriately. However, the defect predictability of the method improves significantly, if the substructure is located close to the defect. Multiple substructures at different locations are expected to work better, since at least one of them is likely to be close to the location of defect. As in all engineering problems, engineering judgment is expected to improve the damage predictability of the method. Although for a class of problems, substructuring can be automated, but this option is not considered while developing a general-purpose procedure.

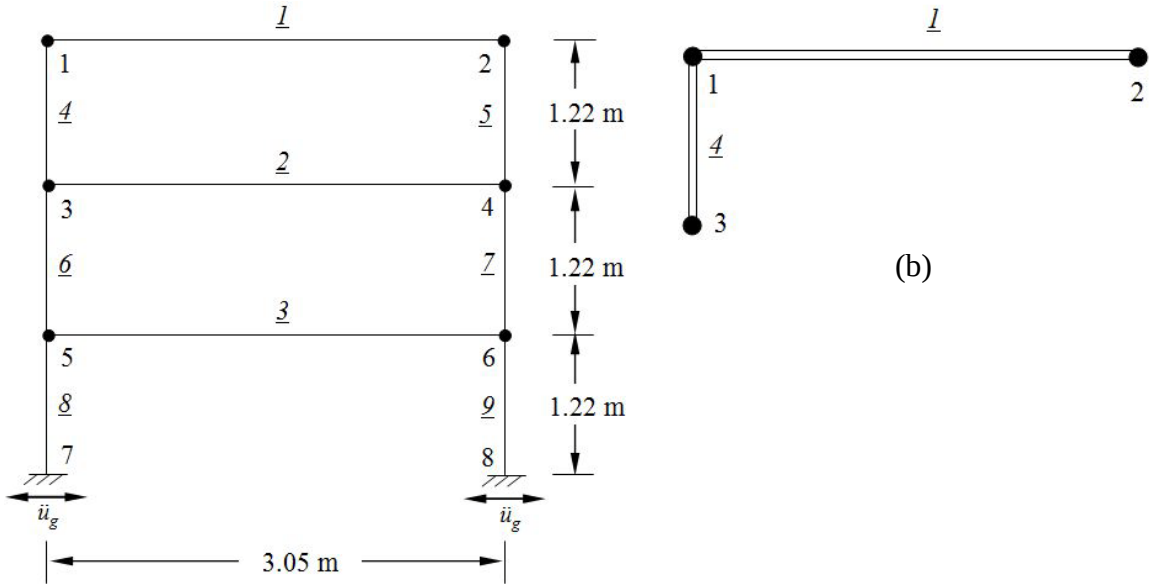

Fig. 2 (a) Finite-element representation of the experimental frame; (b) Substructure for the GILS-EKF-UI method

In order to apply the GILS-EKF-UI method, the state vector can be defined as

$$\{Z(t)\} = \begin{Bmatrix} \{Z_1(t)\} \\ \{Z_2(t)\} \\ \{Z_3(t)\} \end{Bmatrix} = \begin{Bmatrix} \{X(t)\} \\ \{\dot{X}(t)\} \\ \{\tilde{K}\} \end{Bmatrix} \tag{7}$$

where $\{Z(t)\}$ is the state vector at the time *t*, $\{X(t)\}$ and $\{\dot{X}(t)\}$ are the displacement and velocity vectors, respectively, at the time *t* for the whole structure, and $\{\tilde{K}\}$ is a vector containing the stiffness parameters of the whole structure that needs to be identified. The stiffness parameter for the *i*th member, defined earlier for the MILS-UI method as $k_i = E_i I_i / L_i$, will remain the same. The structural system is considered to be time invariant during the identification process; hence, the stiffness parameters $k_1, k_2, \ldots$ will remain unchanged during this period. During the updating process, the derivatives of the state vector are necessary. For seismic excitation, those can be shown to be

$$\begin{aligned} \{\dot{Z}(t)\} &= \begin{Bmatrix} \{\dot{Z}_1(t)\} \\ \{\dot{Z}_2(t)\} \\ \{\dot{Z}_3(t)\} \end{Bmatrix} = \begin{Bmatrix} \{\dot{X}(t)\} \\ \{\ddot{X}(t)\} \\ \{0\} \end{Bmatrix} \\ &= \begin{bmatrix} \{\dot{X}(t)\} \\ -[M]^{-1}\left([K]\{X(t)\} + (\alpha[M] + \beta[K])\{\dot{X}(t)\} + [M]\{I\}\{\ddot{u}_g\}\right) \\ \{0\} \end{bmatrix} \end{aligned} \tag{8}$$

To consider the error in the initial state vector $\{Z_{t_0}\}$, it is considered to be Gaussian with the mean vector $\{\hat{Z}_{t_0}\}$ and the constant error covariance matrix $[P_{t_0}]$, and denoted as $\{Z_{t_0}\} \sim N(\{\hat{Z}_{t_0}\}, [P_{t_0}])$.

To consider uncertainty in the measured responses, the observational vector $\{Y_{t_k}\}$ at the time t_k can be expressed as

$$\{Y_{t_k}\} = [H]\{Z_{t_k}(t_k)\} + \{V_{t_k}\} \tag{9}$$

where $[H]$ is a matrix containing information on the measured responses and $\{V_{t_k}\}$ is the observational noise vector. The vector $\{V_{t_k}\}$ is generally assumed to be Gaussian white noise with zero vector as the mean vector and $[R_{t_k}]$ as the covariance matrix, and denoted as $\{V_{t_k}\} \sim N(\{0\}, [R_{t_k}])$. All the other parameters are same as defined earlier.

1. Stage 1

The substructure used in this study to identify the whole frame is shown in Figure 2(b). The information on the measured response of the frame will satisfy the minimum requirements for implementing the MILS-UI method. A successful completion of Stage 1 will produce information on the stiffness parameters of the two members, i.e., one beam and one column, the unknown excitation and the two Rayleigh damping coefficients. In order to develop the initial state vector of the whole frame, the initial stiffness parameters of all the beams in the frame will be assumed to have the same value as identified for the beam in the substructure. Similarly, all the columns will be assigned the same stiffness parameter as identified for the column in the substructure. With this, the information necessary to implement Stage 2 will become available.

2. Stage 2

With the initial state vector $\{\hat{Z}_0(t_0/t_0)\}$ having been defined at the completion of Stage 1, Stage 2 is initiated with the following steps.

2.1 Step 1: Define the Initial Covariance Matrix

The initial error covariance matrix $[P(t_0/t_0)]$ contains the information on the errors in the measured responses and in the initial estimate of the stiffness parameters of the elements. This is generally expressed as (Hoshiya and Saito, 1984; Wang and Haldar, 1997)

$$[P(t_0/t_0)] = \begin{bmatrix} [P_x(t_0/t_0)] & [0] \\ [0] & [P_k(t_0/t_0)] \end{bmatrix} \tag{10}$$

where $[P_x(t_0/t_0)]$ is a $2n \times 2n$ matrix, which contains the initial covariance matrices of displacement and velocity and is assumed to have a value of 1.0 in the diagonals, and $[P_k(t_0/t_0)]$ is a $ne \times ne$ diagonal matrix, which contains the initial covariance matrix of $\{\tilde{K}\}$. Here, n and ne are the total number of DDOFs and the total number of elements in the whole structure, respectively. Hoshiya and Saito (1984) pointed out that the diagonals in $[P_k(t_0/t_0)]$ should be large positive numbers to accelerate the convergence and recommended the value of 1000 for this purpose.

2.2 Step 2: Prediction Phase

In the context of EKF, the predicted state $\{\hat{Z}(t_{k+1}/t_k)\}$ and its error covariance $[P(t_{k+1}/t_k)]$ for the next time increment is evaluated as

$$\{\hat{Z}(t_{k+1}/t_k)\} = \{\hat{Z}(t_k/t_k)\} + \int_{t_k}^{t_{k+1}} f\left[\{\hat{Z}(t/t_k)\}, t\right] \mathrm{d}t \tag{11}$$

and

$$\left[P\left(t_{k+1}/t_k\right)\right]=\left[\Phi\left[t_{k+1},t_k;\left\{\hat{Z}\left(t_k/t_k\right)\right\}\right]\right]\bullet\left[P\left(t_k/t_k\right)\right]\bullet\left[\Phi\left[t_{k+1},t_k;\left\{\hat{Z}\left(t_k/t_k\right)\right\}\right]\right]^{\mathrm{T}} \tag{12}$$

where the integral in Equation (11) contains the first derivative of the state vector; $\left[\Phi\left[t_{k+1},t_k;\left\{\hat{Z}\left(t_k/t_k\right)\right\}\right]\right]$ is the state transfer matrix from the time t_k to t_{k+1} and can be written in an approximate form as

$$\left[\Phi\left[t_{k+1},t_k;\left\{\hat{Z}\left(t_k/t_k\right)\right\}\right]\right]=\left[I\right]+\Delta t\bullet\left[F\left[t_k;\left\{\hat{Z}\left(t_k/t_k\right)\right\}\right]\right] \tag{13}$$

In this equation, $\left[I\right]$ is a unit matrix and

$$\left[F\left[t_k;\left\{\hat{Z}\left(t_k/t_k\right)\right\}\right]\right]=\left[\frac{\partial f\left[\left\{Z\left(t_k\right)\right\},t_k\right]}{\partial Z_j}\right]_{\left\{Z\left(t_k\right)\right\}=\left\{\hat{Z}\left(t_k/t_k\right)\right\}} \tag{14}$$

where Z_j is the *j*th component of the vector $\left\{Z\left(t_k\right)\right\}$.

2.3 Step 3: Estimation of Kalman Gain

The Kalman gain matrix is estimated in the following way:

$$\begin{aligned}\left[K\left[t_{k+1};\left\{\hat{Z}\left(t_{k+1}/t_k\right)\right\}\right]\right]&=\left[P\left(t_{k+1}/t_k\right)\right]\bullet\left[M\left[t_{k+1};\left\{\hat{Z}\left(t_{k+1}/t_k\right)\right\}\right]\right]^{\mathrm{T}}\\&\bullet\left\{\left[M\left[t_{k+1};\left\{\hat{Z}\left(t_{k+1}/t_k\right)\right\}\right]\right]\bullet\left[P\left(t_{k+1}/t_k\right)\right]\bullet\left[M\left[t_{k+1};\left\{\hat{Z}\left(t_{k+1}/t_k\right)\right\}\right]\right]^{\mathrm{T}}+\left[R\left(t_{k+1}\right)\right]\right\}^{-1}\end{aligned} \tag{15}$$

with

$$\left[M\left[t_k;\left\{\hat{Z}\left(t_k/t_k\right)\right\}\right]\right]=\frac{\partial\left[H\left(\left\{Z\left(t_k\right)\right\},t_k\right)\right]}{\partial Z_j} \tag{16}$$

2.4 Step 4: Updating Phase

Since observations are available at the time t_{k+1}, the updated state $\left\{\hat{Z}\left(t_{k+1}/t_{k+1}\right)\right\}$ is obtained by using the Kalman gain matrix $\left[K\left[t_{k+1};\left\{\hat{Z}\left(t_{k+1}/t_k\right)\right\}\right]\right]$ and by using the information on the predicted state (via Equation (11)) and the observed state as

$$\left\{\hat{Z}\left(t_{k+1}/t_{k+1}\right)\right\}=\left\{\hat{Z}\left(t_{k+1}/t_k\right)\right\}+\left[K\left[t_{k+1};\left\{\hat{Z}\left(t_{k+1}/t_k\right)\right\}\right]\right]\bullet\left\{\left[Y\left(t_{k+1}\right)\right]-\left[H\left(\left\{\hat{Z}\left(t_{k+1}/t_k\right)\right\}\right)\right]\right\} \tag{17}$$

The corresponding updated error covariance matrix $\left[P\left(t_{k+1}/t_{k+1}\right)\right]$ can be shown to be

$$\begin{aligned}\left[P\left(t_{k+1}/t_{k+1}\right)\right]&=\left\{\left[I\right]-\left[K\left[t_{k+1};\left\{\hat{Z}\left(t_{k+1}/t_k\right)\right\}\right]\right]\bullet\left[M\left[t_{k+1};\left\{\hat{Z}\left(t_{k+1}/t_k\right)\right\}\right]\right]\right\}\bullet\left[P\left(t_{k+1}/t_k\right)\right]\\&\bullet\left\{\left[I\right]-\left[K\left[t_{k+1};\left\{\hat{Z}\left(t_{k+1}/t_k\right)\right\}\right]\right]\bullet\left[M\left[t_{k+1};\left\{\hat{Z}\left(t_{k+1}/t_k\right)\right\}\right]\right]\right\}^{\mathrm{T}}\\&+\left[K\left[t_{k+1};\left\{\hat{Z}\left(t_{k+1}/t_k\right)\right\}\right]\right]\bullet\left[R\left(t_{k+1}\right)\right]\bullet\left[K\left[t_{k+1};\left\{\hat{Z}\left(t_{k+1}/t_k\right)\right\}\right]\right]^{\mathrm{T}}\end{aligned} \tag{18}$$

The prediction and updating will continue for every time increment, i.e., when *k* is replaced by *k*+1. The process will continue until all the time points are used, i.e., *k* becomes equal to *m*, where *m* represents the total number of discrete time points of the measurements. The iteration process covering all the time points is generally denoted as local iteration. However, the identified parameters obtained through the

local iteration may not be stable and convergent. To obtain the desired results, a weighted global iteration procedure, suggested by Hoshiya and Saito (1984), can be used. To accomplish this, a weight factor *w* is introduced in the error covariance matrix for the stiffness parameters to be estimated in Equation (10), and the same prediction and updating steps are carried out for all the *m* time points. Hoshiya and Saito (1984) reported that weight factor played an important role to promote convergence, although it may lead to fluctuations in the state vector in first few iterations. Hoshiya and Saito (1984), Koh et al. (1991), Oreta and Tanabe (1993, 1994) assumed *w* to be 100. Hoshiya and Sutoh (1993) assumed it to be in the range of 1000 to 10000 in some applications. In a more recent work, Ghosh et al. (2007) assumed *w* to be 100. In this study *w* is considered to be 100 or 1000, depending on the application.

The overall process to implement Stage 2 of the GILS-EKF-UI method can be described as follows. Stage 2 is initiated by assuming the initial state vector $\left\{\hat{Z}_0\left(t_0/t_0\right)\right\}$ and error covariance matrix $\left[P\left(t_0/t_0\right)\right]$. At the completion of the local iteration, updated information on the corresponding terms, denoted as $\left\{\hat{Z}^{(1)}\left(t_m/t_m\right)\right\}$ and $\left[P^{(1)}\left(t_m/t_m\right)\right]$ respectively, will be available. Here, the superscript (1) denotes the first global iteration. To initiate the 2nd global iteration, $\left\{\hat{Z}^{(2)}\left(t_0/t_0\right)\right\}$ and $\left[P^{(2)}\left(t_0/t_0\right)\right]$ need to be assumed, say equal to $\left\{\hat{Z}^{(1)}\left(t_m/t_m\right)\right\}$ and $w\left[P^{(1)}\left(t_m/t_m\right)\right]$, respectively. On the completion of this iteration, the information on $\left\{\hat{Z}^{(2)}\left(t_m/t_m\right)\right\}$ and $\left[P^{(2)}\left(t_m/t_m\right)\right]$ will become available. The global iteration process will continue, until a predetermined convergence criterion is satisfied for the identified structural parameters, i.e., $\left\|\left[K^{(i)}\left(t_m/t_m\right)\right]-\left[K^{(i-1)}\left(t_m/t_m\right)\right]\right\| \le \varepsilon$, where i represents the global iteration number and ε is the acceptable tolerance level. Since the stiffness parameters in this study are of the order of 100000, ε is considered to be between 10 and 100. In some cases, convergence may not be achieved. In those cases, the minimization of an objective function $\bar{\theta}$ will be necessary (Hoshiya and Saito, 1984). However, this is beyond the scope of this paper. In any case, after the completion of Stage 2, the whole structure is identified by using the response information measured only at the substructure.

EXAMPLE: HEALTH ASSESSMENT OF A 2-D FRAME EXCITED BY EARTHQUAKE GROUND MOTION

A three-story, single-bay, two-dimensional, steel frame shown in Figure 1 is considered to verify the MILS-UI and GILS-EKF-UI methods. The same frame has already been tested in laboratory by exciting it with the sinusoidal and impulsive forces (Martinez-Flores, 2005). The health assessments of defect-free and defective frames by using experimental response information have also been published for this case (Martinez-Flores, 2005; Martinez-Flores and Haldar, 2007; Martinez-Flores et al., 2008).

For completeness in this paper, a brief discussion on the example frame is necessary. This frame has been designed according to the design guidelines of American Institute of Steel Construction's (AISC's) LRFD Manual and scaled to one-third of its actual dimensions to fit the testing facilities. The scaled frame has the bay width of 3.05 m and the story height of 1.22 m. The frame consists of nine members, i.e., six columns and three beams. The steel section of size S4x7.7 has been used for all the beams and columns in order to minimize the effects of fabrication defects and differences in the material properties. Assuming that the bases are fixed, the frame can be represented by 18 DDOFs. The nominal cross-sectional properties of the chosen section are available from any standard steel manual. However, before testing the frame in laboratory, the scenarios considered have been studied analytically in an exhaustive manner. The actual values of cross-sectional area, mass, moment of inertia and damping properties are expected to be different from the nominal values and are therefore determined first as discussed next.

1. Estimation of Actual Cross-Sectional Area

Martinez-Flores (2005) conducted a simple experiment to establish the actual cross-sectional area of the members of the example frame. A test specimen was submerged into a container filled with water, and

by using the information on the displaced water, the average cross-sectional area of the specimen members was estimated to be 14.14 cm^2. This is less than 3% of the nominal value, and hence, in developing the analytical model the estimated area of 14.14 cm^2 is considered.

2. Estimation of Moment of Inertia

A trial and error method is used to calculate the actual moment of inertia of the structural members. The defect-free frame was excited by a sinusoidal load and acceleration time history was recorded at the top of the frame at Node 2. By using the fast Fourier transform (FFT), the first two natural frequencies were estimated to be f_1 = 9.76 Hz and f_2 = 34.12 Hz. A theoretical finite-element model of the frame was also developed by considering the area of the elements same as that estimated experimentally. The Young's modulus of elasticity of the material was taken as 123.3×10^9 N/m^2. The moment of inertia of the elements was changed so that there was matching between the first two natural frequencies of the experimental and theoretical models. Reasonably good matching was observed between the experimental and theoretical frequencies, when the nominal moment of inertia was reduced by 6%. Therefore, the actual moment of inertia is estimated to be 94% of the nominal moment of inertia, i.e., equal to $0.94\times253.9 = 238.7$ cm^4.

3. Estimation of Mass

As mentioned above, all the beams and columns have the same cross-sectional area. Hence, to estimate their mass, they are simply weighed and the mass is estimated to be 11.5 kg/m.

4. Estimation of Damping

The logarithmic decrement method is employed to evaluate the amount of viscous damping present in the frame and the damping coefficient ξ for the frame is estimated based on the rate of decay of the oscillatory response of the structure (Clough and Penzien, 1993). The frame was excited by an impulsive load and the acceleration time history at the roof at Node 1 was recorded. This time history was then post-processed and integrated twice to obtain the displacement time history. Assuming damping to be same in the first two modes and following the procedure suggested by Clough and Penzien (1993), the corresponding (problem-specific) Rayleigh damping coefficients are estimated.

5. Generation of Theoretical Responses and Health Assessment of the Frame

The actual stiffness values, $k_i = E_i I_i / L_i$, i = 1, 2, …, are found to be 96500 N-m for all the beams and 241250 N-m for all the columns. To simulate the gravity load, a uniformly distributed load of 3675 N/m is applied on all the floor beams. The first two natural frequencies of the frame are estimated to be 2.0915 and 7.3063 Hz, and the Rayleigh damping coefficients α and β are estimated to be 0.245404 and 0.000406786, respectively. The analytical responses of the defect-free frame have been evaluated by using ANSYS, Version 11, a commercially available computer program, for excitation by the recorded acceleration time history of 1994 El Centro earthquake shown in Figure 3.

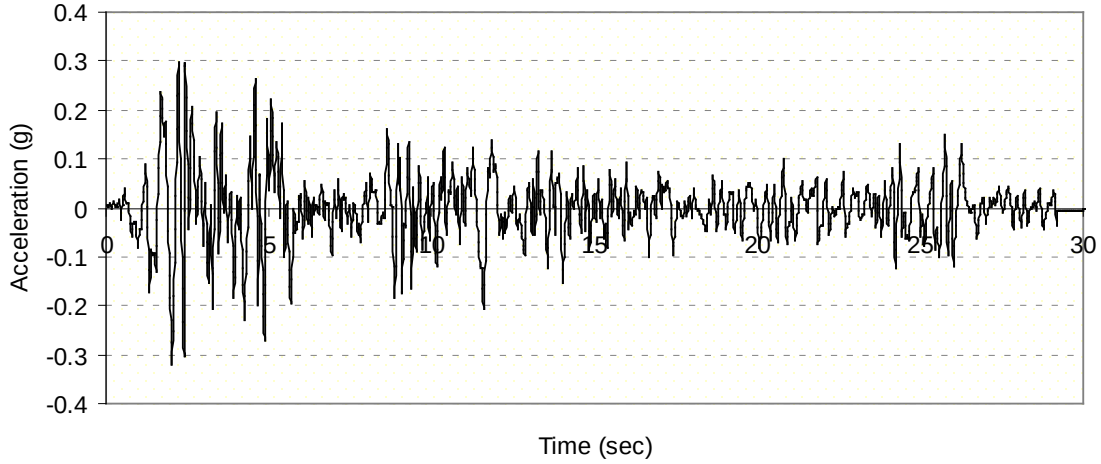

Fig. 3 1994 El Centro earthquake acceleration time history

The displacement, velocity, and acceleration time histories are calculated at each DDOF for the time increment of 0.00025 s for a total duration of 3 s. To consider the defective state of the frame, three scenarios of this state are considered. For the purpose of discussion and on referring to Figure 2(a), these scenarios are (i) Beam 1 is broken, (ii) Beam 2 is broken, and (iii) Beam 3 is broken. To obtain analytical responses for these scenarios, the moment of inertia of the broken beams is considered to be 0.1% of that in the defect-free state. Again, ANSYS, Version 11 is used to estimate the responses at all DDOFs under the same seismic excitation for each scenario. Once the responses have been obtained for both defect-free and defective states, those are considered to be the measured responses and the information on input seismic excitation is completely ignored for the purpose of structural health assessment. It is important to note that the initial finite element representation of the defect-free frame is not changed for the defective states. Therefore, the task is whether the MILS-UI and GILS-EKF-UI methods can identify the locations and severity of defects.

6. Health Assessment of Defect-Free Frame Using the MILS-UI Method

Although theoretical responses are available for a longer duration, the responses between 1.52 and 2.37 s with a sampling interval of 0.01 s are used. While using the responses for all the 18 DDOFs, the stiffness parameters for all the nine members of the defect-free frame are identified by using the MILS-UI method. The identified stiffness parameters are summarized in Table 1. On comparing the identified stiffness parameters with their expected or analytical values, the errors in the identification are found to be very small, i.e., of the order of 0.002%, for all the members. Since the stiffness parameters did not change among all the members, the frame is identified to be defect-free. This indicates that the MILS-UI method accurately identifies the defect-free state of the frame for the seismic excitation considered.

Table 1: Stiffness Parameter Identification for Defect-Free Frame Using MILS-UI Method

Member i	**Stiffness Parameter k_i $(= E_i I_i / L_i)$ Values**		
	Nominal (N-m)	**Identified (N-m)**	**Error (%)**
(1)	(2)	(3)	(4)
1	96500	96498	−0.002
2	96500	96498	−0.002
3	96500	96498	−0.002
4	241250	241244	−0.002
5	241250	241244	−0.002
6	241250	241244	−0.002
7	241250	241244	−0.002
8	241250	241244	−0.002
9	241250	241244	−0.002

7. Health Assessment for Defective Frame Using the MILS-UI Method

After successfully identifying the defect-free frame, the three scenarios of the defective state of the frame are considered one at a time. For a broken member, its stiffness parameter is supposed to be zero, with the understanding that it is impractical to obtain a zero value for this parameter numerically. Similar to the case of defect-free frame, on using the responses for all the 18 DDOFs between 1.52 and 2.37 s with the sampling interval of 0.01 s, the stiffness parameters for all the members are identified for the three defective states by using the MILS-UI method. The results of identification are summarized in Table 2.

For all the three scenarios of the defective state, the identified stiffness parameters for the broken members are found to be of the order of 100 N-m, as compared to the value of 96500 N-m for the defect-free state of the frame. The stiffness parameters for the other members did not change significantly, thereby indicating the location of the defect. For the three scenarios of the defective state, it is thus found that the MILS-UI method correctly identifies the locations and severity of the defects in the case of seismic excitations.

Table 2: Stiffness Parameter Identification for Broken Members Using MILS-UI Method

Member i	Stiffness Parameter k_i $(= E_i I_i / L_i)$ Values (N-m)			
	Nominal	Identified		
		Broken Beam 1	Broken Beam 2	Broken Beam 3
(1)	(2)	(3)	(4)	(5)
1	96500	100	96588	96571
2	96500	96560	101	96574
3	96500	96562	96595	100
4	241250	241400	241473	241430
5	241250	241400	241473	241430
6	241250	241405	241488	241436
7	241250	241405	241488	241436
8	241250	241406	241491	241440
9	241250	241406	241491	241440

8. Health Assessment for Defect-Free Frame Using GILS-EKF-UI Method

While considering the substructure shown in Figure 2(b) and using only the responses at its 9 DDOFs, the whole defect-free frame is identified by using the GILS-EKF-UI method. Based on the prior experience, the sampling interval is considered to be 0.00025 s to implement the procedure. By using the responses between 1.52 and 2.37 s, the substructure of the defect-free frame is first identified and the results are shown in Table 3(a). These results indicate that the stiffness parameters of the beam and column in the substructure are identified quite accurately in Stage 1. The unknown input ground acceleration is also identified accurately, as shown in Figure 4.

By using the information generated in Stage 1 (based on the responses at 9 DDOFs), the whole frame is identified in Stage 2. The different amounts of noises in the measured responses are considered by changing the diagonal terms of the covariance matrix $\left[R_{t_k} \right]$. The results corresponding to the diagonal values of 10^{-2} and 10^{-4} are summarized in Table 3(b) (see Columns 3 and 4, respectively). As expected, the errors in the identification are observed to go up with an increase in the noise level in the responses.

It is obvious that the total number of responses used to identify a structure will determine the accuracy in the predictions. For seismic excitations, the horizontal responses are expected to control the structural behavior and therefore the stiffness parameters are identified again by additionally considering the horizontal responses at Nodes 4, 5 and 6 (in addition to the responses at the 9 DDOFs of the substructure). The identified stiffness parameters for all the members are given in Table 3(b) (see Columns 5 and 6 for the diagonal terms of 10^{-2} and 10^{-4}, respectively, in the covariance matrix $\left[R_{t_k} \right]$). The corresponding maximum errors in the stiffness parameter identification are found to be 3.6% and 3.05%, respectively. This exercise clearly indicates the value of considering additional responses; the cost may go up but predictability will be improved. Further, it is observed that the identified stiffness parameters do not change significantly from member to member, which indicates that the frame is defect-free.

9. Health Assessment for Defective Frame Using GILS-EKF-UI Method

Considering the same three scenarios of the defective state as discussed earlier and the responses measured between 1.52 and 2.37 s with the sample interval of 0.00025 s, the frame is identified. It may be noted that for the first scenario, the substructure contains the defect. Table 4(a) shows that the identified results for Stage 1 are very accurate for all the three scenarios. The results for the identified stiffness parameters for the whole frame, as obtained by using the responses at the 12 DDOFs, are shown in Table 4(b). In some cases, the identified stiffness parameters for the broken members are observed to be negative, and in all cases, they are very small, thus indicating the locations and severity of defects. The identified results for the first scenario clearly indicate that the defect has been identified more accurately. This observation suggests that the proximity of the defect to the substructure may be an important defect identification parameter. This needs to be investigated more extensively. In any case, the locations and

severity of the defects in all the three cases have been identified correctly for the seismic excitations also. This study thus confirms that the GILS-EKF-UI method is robust and that this can identify structural health for different types of excitations.

Table 3: Stiffness Parameter Identification for Defect-Free Frame Using GILS-EKF-UI Method: (a) Stage 1—Substructure Identification; (b) Stage 2—Identification of Whole Structure

(a)			
Member *i*	**Stiffness Parameter k_i $(= E_i I_i / L_i)$ Values**		
	Nominal (N-m)	**Identified (N-m)**	**Error (%)**
(1)	(2)	(3)	(4)
1	96500	96498	−0.002
4	241250	241244	−0.002

(b)					
Member *i*	**Stiffness Parameter k_i $(= E_i I_i / L_i)$ Values (N-m)**				
	Nominal	**Identified**			
		9 DDOFs		**12 DDOFs**	
		Diagonal $\left[R_{t_k}\right]$ Value $= 10^{-2}$	**Diagonal $\left[R_{t_k}\right]$ Value $= 10^{-4}$**	**Diagonal $\left[R_{t_k}\right]$ Value $= 10^{-2}$**	**Diagonal $\left[R_{t_k}\right]$ Value $= 10^{-4}$**
(1)	(2)	(3)	(4)	(5)	(6)
1	96500	102005	96946	97216	96225
2	96500	84888	94334	95123	96893
3	96500	111356	79379	98044	94840
4	241250	250776	229117	241853	237739
5	241250	277351	238014	245891	239033
6	241250	118007	182932	233237	242091
7	241250	176952	208766	249935	248598
8	241250	172766	496563	238373	247199
9	241250	431023	165941	239774	240178

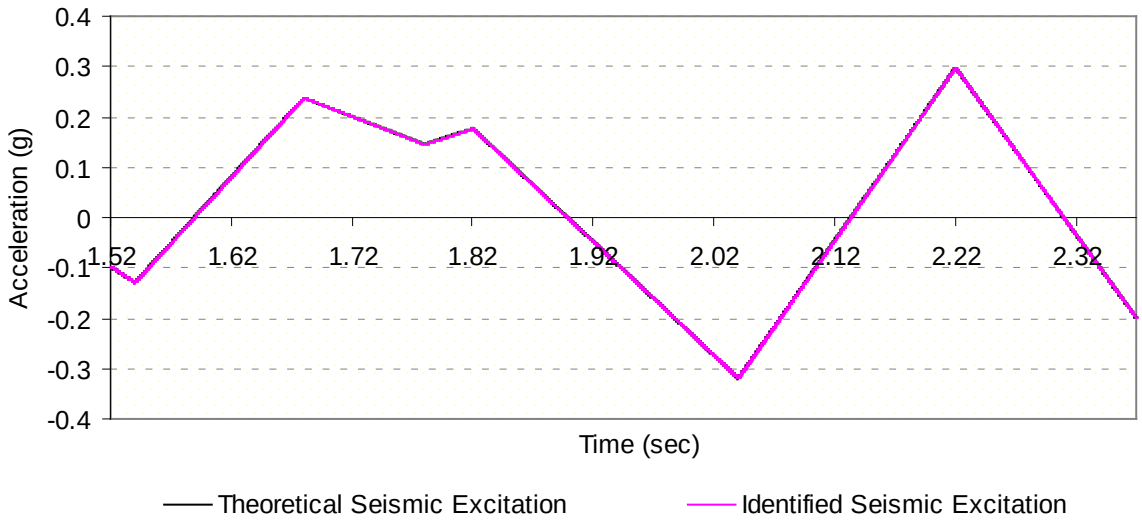

Fig. 4 Theoretical and identified seismic excitations

Table 4: Stiffness Parameter Identification for Broken Members Using GILS-EKF-UI Method: (a) Stage 1—Substructure Identification; (b) Stage 2—Identification of Whole Structure

(a)

Member i	Stiffness Parameter k_i $(= E_i I_i / L_i)$ Values						
	Nominal (N-m)	Broken Beam 1		Broken Beam 2		Broken Beam 3	
		Identified (N-m)	Error (%)	Identified (N-m)	Error (%)	Identified (N-m)	Error (%)
(1)	(2)	(3)	(4)	(5)	(6)	(7)	(8)
1	96500	100	−99.896	96498	−0.002	96498	−0.002
4	241250	241410	0.066	241244	−0.002	241245	−0.002

(b)

Member i	Stiffness Parameter k_i $(= E_i I_i / L_i)$ Values (N-m)						
	Nominal	Identified					
		Broken Beam 1		Broken Beam 2		Broken Beam 3	
		Diagonal $\left[R_{t_k}\right]$ Value $= 10^{-2}$	Diagonal $\left[R_{t_k}\right]$ Value $= 10^{-4}$	Diagonal $\left[R_{t_k}\right]$ Value $= 10^{-2}$	Diagonal $\left[R_{t_k}\right]$ Value $= 10^{-4}$	Diagonal $\left[R_{t_k}\right]$ Value $= 10^{-2}$	Diagonal $\left[R_{t_k}\right]$ Value $= 10^{-4}$
(1)	(2)	(3)	(4)	(5)	(6)	(7)	(8)
1	96500	−66	442	94845	94798	98561	95194
2	96500	96733	95985	1030	1034	93255	98702
3	96500	97431	96235	94740	94778	2415	−2104
4	241250	243439	236935	235530	234816	243379	236311
5	241250	243945	237021	233756	233889	253192	233666
6	241250	236679	240039	233788	236803	227883	245882
7	241250	242972	245101	248438	245556	253281	240446
8	241250	226651	250292	245453	249306	230783	250677
9	241250	253244	234827	244920	241031	235759	248391

CONCLUSIONS

Conceptual bases for the two vibration-based structural health assessment procedures, denoted as MILS-UI and GILS-EKF-UI methods, under development by the research team at the University of Arizona have been presented. Both procedures were analytically and experimentally verified in the past for the sinusoidal and impulsive excitations. They have been analytically verified for the seismic excitations by using the numerically generated response information in this paper to establish their robustness. Both methods are finite-element based and use dynamic response information to identify the defective elements. The MILS-UI method is considered to be more appropriate for the SHA of small systems. Since the GILS-EKF-UI method can assess structural health by using the responses measured at limited locations in the structure, it is considered to be more appropriate for large structural systems. This study also indicates that the selection of the location of the substructure is an important parameter to identify defects. Hence, for large structural systems, multiple substructures may be necessary. This needs to be investigated further. Nevertheless, this study confirms the robustness of both the procedures and indicates great implementation potential of these procedures to assess the structural health of real structures.

REFERENCES

1. Ahmed, N.H. (2009). "Dynamic State Estimation Techniques for Identification of Parameters of Finite Element Structural Models", Ph.D. Thesis, Department of Civil Engineering, Indian Institute of Science, Bangalore.
2. Clough, R.W. and Penzien, J. (1993). "Dynamics of Structures", McGraw-Hill, Inc., New York, U.S.A.
3. Corigliano, A. and Mariani, S. (2004). "Parameter Identification in Explicit Structural Dynamics: Performance of the Extended Kalman Filter", Computer Methods in Applied Mechanics and Engineering, Vol. 193, No. 36-38, pp. 3807–3835.
4. Doebling, S.W., Farrar, C.R., Prime, M.B. and Shevitz, D.W. (1996). "Damage Identification and Health Monitoring of Structural and Mechanical Systems from Changes in Their Vibration Characteristics: A Literature Review", Report LA-13070-MS, Los Alamos National Laboratory, Los Alamos, U.S.A.
5. Ghanem, R. and Ferro, G. (2006). "Health Monitoring for Strongly Non-linear Systems Using the Ensemble Kalman Filter", Structural Control and Health Monitoring, Vol. 13, No. 1, pp. 245–259.
6. Ghanem, R. and Shinozuka, M. (1995). "Structural-System Identification. I: Theory", Journal of Engineering Mechanics, ASCE, Vol. 121, No. 2, pp. 255–264.
7. Ghosh, S.J., Roy, D. and Manohar, C.S. (2007). "New Forms of Extended Kalman Filter via Transversal Linearization and Applications to Structural System Identification", Computer Methods in Applied Mechanics and Engineering, Vol. 196, No. 49-52, pp. 5063–5083.
8. Haldar, A. (2009). "Structural Health Assessment Using Noise-Contaminated Minimum Dynamic Response Information" in "Frontier Technologies for Infrastructures Engineering (edited by S.-S. Chen and A.H.-S. Ang)", CRC Press/Balkema, Leiden, The Netherlands.
9. Haldar, A. and Das, A.K. (2010). "Prognosis of Structural Health–Nondestructive Methods", International Journal of Performability Engineering, Vol. 6, No. 5, pp. 487–498.
10. Haldar, A., Martinez-Flores, R. and Katkhuda, H. (2008). "Crack Detection in Existing Structures Using Noise-Contaminated Dynamic Responses", Theoretical and Applied Fracture Mechanics, Vol. 50, No. 1, pp. 74–80.
11. Hoshiya, M. and Saito, E. (1984). "Structural Identification by Extended Kalman Filter", Journal of Engineering Mechanics, ASCE, Vol. 110, No. 12, pp. 1757–1770.
12. Hoshiya, M. and Sutoh, A. (1993). "Kalman Filter—Finite Element Method in Identification", Journal of Engineering Mechanics, ASCE, Vol. 119, No. 2, pp. 197–210.
13. Housner, G.W., Bergman, L.A., Caughey, T.K., Chassiakos, A.G., Claus, R.O., Masri, S.F., Skelton, R.E., Soong, T.T., Spencer, B.F. and Yao, J.T.P. (1997). "Structural Control: Past, Present, and Future", Journal of Engineering Mechanics, ASCE, Vol. 123, No. 9, pp. 897–971.
14. Humar, J., Bagchi, A. and Xu, H. (2006). "Performance of Vibration-Based Techniques for the Identification of Structural Damage", Structural Health Monitoring, Vol. 5, No. 3, pp. 215–241.
15. Jazwinski, A.H. (1970). "Stochastic Processes and Filtering Theory", Academic Press, Inc., New York, U.S.A.
16. Katkhuda, H.N. (2004). "In-Service Health Assessment of Real Structures at the Element Level with Unknown Input and Limited Global Responses", Ph.D. Dissertation, Department of Civil Engineering and Engineering Mechanics, University of Arizona, Tucson, U.S.A.
17. Katkhuda, H. and Haldar, A. (2006). "Defect Identification under Uncertain Blast Loading", Optimization and Engineering, Vol. 7, No. 3, pp. 277–296.
18. Katkhuda, H. and Haldar, A. (2008). "A Novel Health Assessment Technique with Minimum Information", Structural Control and Health Monitoring, Vol. 15, No. 6, pp. 821–838.
19. Katkhuda, H., Martinez, R. and Haldar, A. (2005). "Health Assessment at Local Level with Unknown Input Excitation", Journal of Structural Engineering, ASCE, Vol. 131, No. 6, pp. 956–965.
20. Kerschen, G., Worden, K., Vakakis, A.F. and Golinval, J.-C. (2006). "Past, Present and Future of Nonlinear System Identification in Structural Dynamics", Mechanical Systems and Signal Processing, Vol. 20, No. 3, pp. 505–592.

21. Koh, C.G., See, L.M. and Balendra, T. (1991). “Estimation of Structural Parameters in Time Domain: A Substructure Approach”, Earthquake Engineering & Structural Dynamics, Vol. 20, No. 8, pp. 787–801.
22. Lew, J.-S., Juang, J.-N. and Longman, R.W. (1991). “Comparison of Several System Identification Methods for Flexible Structures”, Proceedings of the AIAA/ASME/ASCE/AHS/ASC 32nd Structures, Structural Dynamics, and Materials Conference, Baltimore, U.S.A., pp. 2304–2318.
23. Ling, X. and Haldar, A. (2004). “Element Level System Identification with Unknown Input with Rayleigh Damping”, Journal of Engineering Mechanics, ASCE, Vol. 130, No. 8, pp. 877–885.
24. Martinez-Flores, R. (2005). “Damage Assessment Potential of a Novel System Identification Technique—Experimental Verification”, Ph.D. Dissertation, Department of Civil Engineering and Engineering Mechanics, University of Arizona, Tucson, U.S.A.
25. Martinez-Flores, R. and Haldar, A. (2007). “Experimental Verification of a Structural Health Assessment Method without Excitation Information”, Journal of Structural Engineering, SERC, Vol. 34, No. 1, pp. 33–39.
26. Martinez-Flores, R., Katkhuda, H. and Haldar, A. (2008). “Structural Performance Assessment with Minimum Uncertainty-Filled Information”, International Journal of Performability Engineering, Vol. 4, No. 2, pp. 121–140.
27. Maruyama, O. and Hoshiya, M. (2001). “System Identification of an Experimental Model by Extended Kalman Filter”, Proceedings of the 8th International Conference on Structural Safety and Reliability (ICOSSAR ’01), Newport Beach, U.S.A., Paper No. 12-2 (on CD).
28. Maybeck, P.S. (1979). “Stochastic Models, Estimation, and Control: Volume 1”, Academic Press, Inc., New York, U.S.A.
29. Oreta, A.W.C. and Tanabe, T. (1993). “Localized Identification of Structures by Kalman Filter”, Structural Engineering/Earthquake Engineering, JSCE, Vol. 9, No. 4, pp. 217s–225s.
30. Oreta, A.W.C. and Tanabe, T. (1994). “Element Identification of Member Properties of Framed Structures”, Journal of Structural Engineering, ASCE, Vol. 120, No. 7, pp. 1961–1976.
31. Rytter, A. (1993). “Vibration Based Inspection of Civil Engineering Structures”, Ph.D. Thesis, Department of Building Technology and Structural Engineering, Aalborg University, Aalborg, Denmark.
32. Saha, N. and Roy, D. (2009). “Extended Kalman Filters Using Explicit and Derivative-Free Local Linearizations”, Applied Mathematical Modelling, Vol. 33, No. 6, pp. 2545–2563.
33. Shinozuka, M. and Ghanem, R. (1995). “Structural System Identification. II: Experimental Verification”, Journal of Engineering Mechanics, ASCE, Vol. 121, No. 2, pp. 265–273.
34. Vo, P.H. and Haldar, A. (2003). “Post-processing of Linear Accelerometer Data in Structural Identification”, Journal of Structural Engineering, SERC, Vol. 30, No. 2, pp. 123–130.
35. Vo, P.H. and Haldar, A. (2004). “Health Assessment of Beams—Experimental Investigations”, Journal of Structural Engineering, SERC, Vol. 31, No. 1, pp. 23–30.
36. Vo, P.H. and Haldar, A. (2008a). “Health Assessment of Beams—Theoretical Formulation and Analytical Verification”, Structure and Infrastructure Engineering, Vol. 4, No. 1, pp. 33–44.
37. Vo, P.H. and Haldar, A. (2008b). “Health Assessment of Beams—Experimental Verification”, Structure and Infrastructure Engineering, Vol. 4, No. 1, pp. 45–56.
38. Wang, D. and Haldar, A. (1994). “Element-Level System Identification with Unknown Input”, Journal of Engineering Mechanics, ASCE, Vol. 120, No. 1, pp. 159–176.
39. Wang, D. and Haldar, A. (1997). “System Identification with Limited Observations and without Input”, Journal of Engineering Mechanics, ASCE, Vol. 123, No. 5, pp. 504–511.
40. Welch, G. and Bishop, G. (1995). “An Introduction to the Kalman Filter”, Report TR95-041, Department of Computer Science, University of North Carolina at Chapel Hill, Chapel Hill, U.S.A.
41. Worden, K., Farrar, C.R., Manson, G. and Park, G. (2007). “The Fundamental Axioms of Structural Health Monitoring”, Proceedings of the Royal Society A, Vol. 463, No. 2082, pp. 1639–1664.

42. Worden, K., Farrar, C.R., Haywood, J. and Todd, M. (2008). "A Review of Nonlinear Dynamics Applications to Structural Health Monitoring", Structural Control and Health Monitoring, Vol. 15, No. 4, pp. 540–567.
43. Wu, M. and Smyth, A.W. (2007). "Application of the Unscented Kalman Filter for Real-Time Nonlinear Structural System Identification", Structural Control and Health Monitoring, Vol. 14, No. 7, pp. 971–990.
44. Yang, J.N., Lin, S., Huang, H. and Zhou, L. (2006). "An Adaptive Extended Kalman Filter for Structural Damage Identification", Structural Control and Health Monitoring, Vol. 13, No. 4, pp. 849–867.
45. Yang, J.N., Pan, S. and Huang, H. (2007). "An Adaptive Extended Kalman Filter for Structural Damage Identifications II: Unknown Inputs", Structural Control and Health Monitoring, Vol. 14, No. 3, pp. 497–521.
46. Zhou, L., Wu, S. and Yang, J.N. (2008). "Experimental Study of an Adaptive Extended Kalman Filter for Structural Damage Identification", Journal of Infrastructure Systems, ASCE, Vol. 14, No. 1, pp. 42–51.